

## Zone sculpting using partitioned electrokinetic injections

Max Narovlyansky and George M. Whitesides

*Department of Chemistry and Chemical Biology, Harvard University, 12 Oxford St., Cambridge, Massachusetts 02138, USA*

Todd M. Squires<sup>a)</sup>

*Department of Chemical Engineering, University of California, Santa Barbara, California 93106, USA*

(Received 14 September 2007; accepted 22 October 2007; published online 14 November 2007)

We describe a general and versatile method to sculpt low-dispersion, high-fidelity sample zones in microfluidic devices for high resolution electrokinetic separations. In a simple channel intersection, microfabricated partitions reduce each channel's permittivity to transverse electric fields, yet maintain their permeability to parallel fields. The resulting anisotropy effectively confines fields to the intersection, thus sculpting the injected plug. We demonstrate by injecting narrow yet symmetric sample zones in a poly(dimethylsiloxane) microfluidic device. This simple geometric strategy for sculpting the field and flow lines does not depend on the device material or analyte/electrolyte properties, and is limited in scale only by fabrication capabilities. © 2007 American Institute of Physics. [DOI: 10.1063/1.2814031]

Electrophoretic separations are a workhorse of analytical chemistry. For two species to be clearly resolved in capillary electrophoresis, their corresponding bands must travel sufficiently far that they no longer overlap, but must do so quickly enough that dispersion does not blur the separation. In addition to molecular diffusion, various factors work against the separation process to limit the ultimate resolution: Taylor (convective) dispersion in non-plug flow, Joule heating, intermolecular interactions, and adsorption to walls.<sup>1</sup> Even if such dispersive effects were entirely absent, however, the resolution of the separation could not exceed that given by the width of the initial plug. Reducing the width of this plug, therefore, may decrease the length of time required for separation, decrease the size of the separation device, and increase the ultimate resolution of the separation.

We and others<sup>2-7</sup> are, therefore, interested in developing methods to inject narrow, sharp plugs. The most straightforward technique for injection of a plug involves electrokinetically driving a sample along an injection channel, through an intersection with the separation channel. While simple, this strategy causes the sample to spread into the horizontal channel, yielding an anisotropic, mushroom-shaped plug [Fig. 1(a)] that may lower resolution. A standard remedy involves using a pinched injection, in which additional fields are applied along the horizontal channels to focus the injecting field and yield a steady, trapezoidal sample zone [Fig. 1(b)]. Pinched injections require control over electric fields in all channels connected to the junction, necessitating careful calculation and control, and hindering implementation of this method in large networks of channels. In that regard, neither the double-L<sup>3</sup> nor the double-T<sup>7</sup> geometries alone constitute simple modules for integrated electrokinetic microfluidic devices. Furthermore, pinched injections dispense an asymmetrical band of sample that progressively becomes more triangular with greater pinching (relative strength of horizontal and vertical fields). Using a double-cross isoelectric focusing injection, Fu *et al.*<sup>7</sup> focused the bands in one intersection and injected into a second. The resulting zone in the

second intersection is indeed more symmetric, with nonetheless a small bulge that results from field-line expansion in the open.

Here, we extend these ideas with a simple geometrical strategy that enables one to inject sharp, well-defined sample zones of variable aspect ratio. We do so by addressing the root cause of the sample zone degradation: the expansion of the electric field lines at the intersection of the injection and separation channels [Figs. 2(a) and 2(b)]. Since the plug is defined by the electric field used for injection, sculpting the field lines makes it possible to sculpt the injected plug. Earlier work used microfabricated structures to create synthetic and controllable separation matrices,<sup>8,9</sup> constrictions and inclusions have been employed to reduce dispersion at channel turns,<sup>10</sup> and nanocapillary arrays have been employed as gateable interconnects between channels.<sup>11</sup> Continuing in this vein, we fabricate channels that are highly anisotropic electrically; that is, they are nonpermissive to fields applied perpendicular to the channel, but permissive to parallel fields. This difference in permittivity allows the injection and separation fields to be sculpted, as shown below.

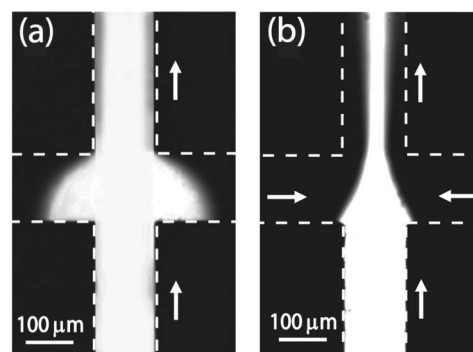


FIG. 1. (a) Distribution of fluorescein (100  $\mu\text{M}$ , in tris-borate-EDTA buffer) using a straightforward electrokinetic injection. Note that analyte spreads into side channels. The white arrows indicate the direction of the electric force acting on the negatively charged molecules. (b) Pinching (isoelectric focusing) fields prevent analyte from spreading into side channels, but yield a nonuniform sample plug.

<sup>a)</sup>Electronic mail: squires@engineering.ucsb.edu

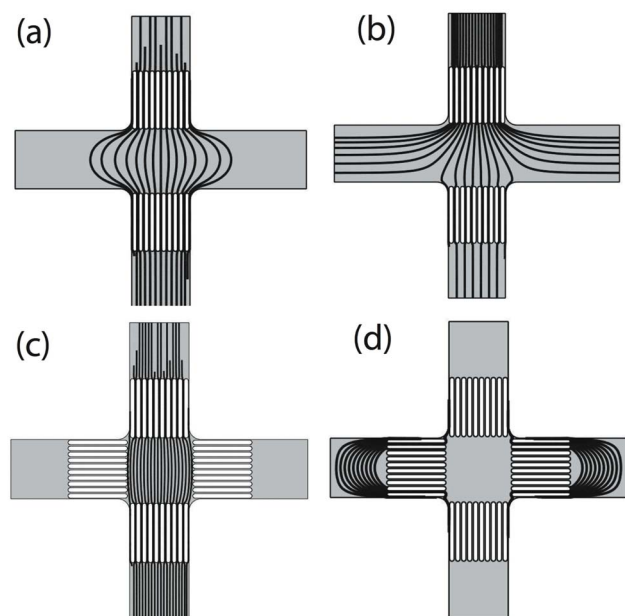


FIG. 2. Electric field lines computed using COMSOL (a) without and (b) with application of lateral focusing potentials. Vertical partitions do not appreciably alter the fields or electrokinetic flows. (c) Horizontal partitions confine the majority of field lines to the channel intersection. (d) A small number of field lines, located near the outer walls of the channel, leak into the horizontal channel.

We must first establish the connection between sculpting electric field lines and sculpting the injected plug. Ions in solution screen charged macromolecules or surfaces over the Debye screening length  $\lambda_D$ , which is typically only a few nanometers thick and thus much smaller than typical channel dimensions. Thus, the electric field in solution obeys Laplace's equation,  $\nabla^2\phi=0$ , with far-field potentials fixed by the electrodes themselves. For impermeable surfaces that neither adsorb molecular species nor permit electrochemical reactions, no ions can be transported into the solid. The steady-state electric field thus satisfies a no-flux condition ( $\hat{n}\cdot\nabla\phi=0$ ) at channel walls, following the formation of a negligibly weak induced screening cloud.<sup>12</sup> Two electrokinetic phenomena typically occur upon application of an electric field  $E$ . Freely suspended analyte particles migrate through the fluid with an electrophoretic velocity  $U=M(\zeta)E$ , where  $\zeta$  is the particle's zeta potential, which forms the basis for open-channel electrophoretic separations. Second, electro-osmotic flows result when the externally applied electric field forces the ionic screening clouds surrounding channel walls into motion. Under fairly general conditions of similitude, electro-osmotic flows are directly proportional, in magnitude and direction, to the electric field lines themselves.<sup>13–15</sup> As such, sample directly follows electric field lines, so that sculpting field lines is tantamount to sculpting the injected plug itself.

Having related field sculpting to plug sculpting, we now describe the use of partitions to inject symmetric sample bands. Using thin microfabricated walls, we partition each channel into a series of thin parallel channels leading up to the intersection of the injection and separation channels. These partitions admit parallel electric fields (and thus electrokinetic transport), with only slight geometric constriction and amplification. Electric field lines perpendicular to the partitions, however, cannot penetrate them due to the no-flux

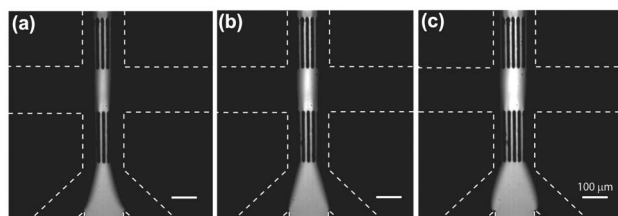


FIG. 3. Fluorescein ( $100\ \mu\text{M}$  in TBE) injected with “sheath” flows restrict analyte to field lines that remain confined to the intersection [Fig. 2(c)]. (a) Strong, (b) medium, and (c) weak sheath flows give narrow, medium, and wide injected zones. All are rectangular, maximizing the injected volume for the given aspect ratio.

condition [Fig. 2(c)]. Numerical computations using COMSOL verify that partitions confine the majority of electric streamlines to the rectangular intersection [Fig. 2(c)], making them more parallel relative to straightforward injections [Fig. 2(a)] and isoelectric focusing [Fig. 2(b)]. Since analyte is transported along field lines and the majority of the analyte remains confined to the intersection, the injected plug has sharper boundaries than plugs in standard injections.

We note as well that depth-averaged pressure-driven flows in shallow channels (Hele-Shaw flows) and electrokinetic flows are *both* governed by Laplace's equation. The former is given by  $\langle u \rangle \propto -\nabla P$ , where the pressure  $P$  obeys  $\nabla^2 P=0$ , whereas the latter is  $u \propto -\nabla\phi$ , where the potential  $\phi$  obeys  $\nabla^2\phi=0$ . Both obey the same no-flux condition at solid walls. In principle, therefore, partitioning will also be effective in sculpting pressure-driven injections.

For field lines to escape the rectangular channel intersection, they must travel the entire length of one partition, across the channel, and back [Fig. 2(d)]. The additional length of the longer paths over which the potential drops reduces both the strength of the unconfined electric fields and the number of field lines taking this path, and increases the field uniformity within the intersection. Simple scaling arguments give estimates for the fraction of the channel that escapes confinement to be  $\Delta w_c/w_c \sim Nw_p/8L$ , where  $N$ ,  $w_p$ , and  $L$  are the number, width, and length of the partitions, respectively. To prevent analyte from leaking through the partitions, sheath flows can be used to confine analyte strictly to field lines that remain confined, and to inject rectangular sample zones of variable width (Fig. 3).

To experimentally test these ideas, we fabricated poly(dimethylsiloxane) microfluidic devices with  $20\ \mu\text{m}$  tall and  $150\ \mu\text{m}$  wide channels using soft lithography.<sup>16</sup> To most easily suppress stray flows during experiments, we introduced a 1.5% agarose solution into a tris-glycine (TG) or tris/borate/ethylenediaminetetraacetic acid (TBE) buffer and let it gel *in situ*, although we obtained similar results without the anticonvective matrix. Using the LabSmith LSV448 for voltage control, we electrokinetically injected sample plugs of  $100\ \mu\text{M}$  fluorescein in TG buffer. Experiments were performed on Nikon TE-2000S microscope with mercury lamp illumination filtered through a Fluorescein isothiocyanate (FITC) filter cube (Chroma) and collected through a  $10\times$  objective (numerical aperture of 0.4) using a General Robotics charge coupled device camera. Further details are described in the Supplemental Information.<sup>17</sup>

Injection of plugs with short axial extent but high sample volume can significantly improve separation resolution. We separated fluorescein and 5-carboxyfluorescein in TG buffer,

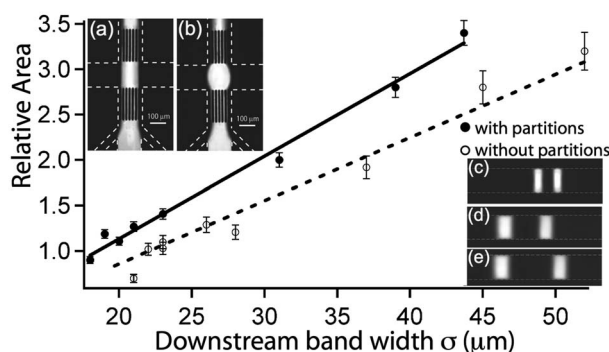


FIG. 4. Sheath flow injections with and without partitions: Fluorescein bands of varying widths were injected, electrophoretically driven down a (perpendicular) separation channel, and imaged  $500\ \mu\text{m}$  downstream. The integrated fluorescence intensity of each band (“relative area”) is plotted against the width  $\sigma$  ( $\mu\text{m}$ ) of the Gaussian profile. Partitioned injections show a consistently greater total intensity than nonpartitioned injections. Insets: Sheath flow injection (a) with partitions and (b) without partitions. [(c)–(e)]. The sample separation of  $100\ \mu\text{M}$  bands of fluorescein and  $5'$  carboxy-fluorescein: (c)  $300\ \mu\text{m}$ , (d)  $500\ \mu\text{m}$ , and (e)  $1000\ \mu\text{m}$  downstream from the partitions.

attaining base line resolution within  $500\ \mu\text{m}$  of the point of injection ( $300\ \mu\text{m}$  after the end of partitions), Figs. 4(c)–4(e). Figure 4 compares the area and width of bands of fluorescein injected with and without partitions; partitions clearly give more sample.

We have demonstrated a simple, geometric method for the electrokinetic injection of well-defined plugs of sample for separations with high resolution and sensitivity. Mushrooming in open-intersection injections leads to a dramatic sample spreading into the separation channel [Fig. 1(a)]. Pinching potentials shape the field, but at the cost of lower injected sample volumes and an asymmetric distribution [Fig. 1(b)]. Our technique uses thin partitions, organized along the axis of two orthogonal channels to establish a highly anisotropic electrical permittivity. The resulting sub-channels remain permissive to longitudinal electric fields, but are impermeable to orthogonal fields. Because the electrokinetically injected sample follows electric field lines, the

injected plug is effectively confined just as the electric field. This method does not depend on fabrication materials or the microchannel size scale (so long as channel features are much larger than  $\lambda_D$ ), is compatible with gel-based separations, and requires only minor design changes for the channels. This simple modification yields symmetric, high aspect-ratio sample zones that may be separated more rapidly and detected more sensitively than with standard injections.

We gratefully acknowledge the support of the NIH (T32-GM07598 and GM065364), the NSF for postdoctoral support under DMS-202550, and NSF CAREER support under CBET-0645097 (TMS).

- <sup>1</sup>J. C. Giddings, *Unified Separation Science* (Wiley, New York, 1991).
- <sup>2</sup>D. J. Harrison, A. Manz, Z. H. Fan, H. Ludi, and H. M. Widmer, *Anal. Chem.* **64**, 1926 (1992).
- <sup>3</sup>C. S. Effenhauser, A. Manz, and H. M. Widmer, *Anal. Chem.* **65**, 2637 (1993).
- <sup>4</sup>S. C. Jacobson, R. Hergenroder, L. B. Koutny, R. J. Warmack, and J. M. Ramsey, *Anal. Chem.* **66**, 1107 (1994).
- <sup>5</sup>S. V. Ermakov, S. C. Jacobson, and J. M. Ramsey, *Anal. Chem.* **72**, 3512 (2000).
- <sup>6</sup>J. P. Alarie, S. C. Jacobson, C. T. Culbertson, and J. M. Ramsey, *Electrophoresis* **21**, 100 (2000).
- <sup>7</sup>L. M. Fu, R. J. Yang, and G. B. Lee, *Anal. Chem.* **75**, 1905 (2003).
- <sup>8</sup>J. O. Tegenfeldt, C. Prinz, H. Cao, R. L. Huang, R. H. Austin, S. Y. Chou, E. C. Cox, and J. C. Sturm, *Anal. Bioanal. Chem.* **378**, 1678 (2004).
- <sup>9</sup>P. S. Doyle, J. Bibette, A. Bancaud, and J. L. Viovy, *Science* **295**, 2237 (2002).
- <sup>10</sup>G. J. Fiechtner and E. B. Cummings, *Anal. Chem.* **75**, 4747 (2003).
- <sup>11</sup>T. C. Kuo, D. M. Cannon, Y. N. Chen, J. J. Tulock, M. A. Shannon, J. V. Sweedler, and P. W. Bohn, *Anal. Chem.* **75**, 1861 (2003).
- <sup>12</sup>T. M. Squires and M. Z. Bazant, *J. Fluid Mech.* **509**, 217 (2004).
- <sup>13</sup>J. L. Anderson, *Annu. Rev. Fluid Mech.* **21**, 61 (1989).
- <sup>14</sup>E. B. Cummings, S. K. Griffiths, R. H. Nilson, and P. H. Paul, *Anal. Chem.* **72**, 2526 (2000).
- <sup>15</sup>J. G. Santiago, *Anal. Chem.* **73**, 2353 (2001).
- <sup>16</sup>J. C. McDonald, D. C. Duffy, J. R. Anderson, D. T. Chiu, H. K. Wu, O. J. A. Schueller, and G. M. Whitesides, *Electrophoresis* **21**, 27 (2000).
- <sup>17</sup>See EPAPS Document No. E-APPLAB-91-021747 for more detailed descriptions of the experimental procedures and simulations. This document can be reached through a direct link in the online article’s HTML reference section or via the EPAPS homepage (<http://www.aip.org/pubservs/epaps/html>).